Original Research Article

Experimental study of the thermal performance of a sensitive solar energy storage system on a rock bed (granite) for a drying application

Abstract

The use of solar energy is hampered by the intermittency of the resource and the constraints of storing the thermal form of this energy. The processes using this resource are therefore faced with problems of continuity of the process. To remedy this, this work proposes to develop a device for the accumulation of solar thermal energy by a sensitive storage system on a rock bed. A solar thermal energy storage system has been developed and experimentally studied with a view to coupling it to a solar dryer. The thermal performance of the system was evaluated in terms of spatial and temporal distribution of bed temperature, total energy stored, total energy discharged, charging efficiency, discharging efficiency and overall storage system efficiency. The results obtained indicate that the stratification in the storage system decreases in the afternoon due to the reduction of solar radiation and the output temperature of the solar collector. This contributes to a decrease in the thermal performance of the storage system. The charging efficiency obtained is 76.8%, the discharging efficiency 44.4%. The results also indicate that out of 4.7 MJ of total stored energy almost 89% or 4.17% was recovered during the discharge phase which is interesting for solar dryers.

Nomenclature

C_{P_a}	Heat capacity of air (J/kg.K)
$C_{p,s}$	Heat capacity of rock (J/kg.K)
d_{eq}	Equivalent diameter (m)
$d_{eq,a}$	Diameter of the sphere with the same specific surface area (m)
E_{Tch}	Stored energy (J)
$\dot{m}_{ch}$	Masse flow rate of charge (kg/s)
$\dot{m}_{dech}$	Masse flow rate of discharge (kg/s)
m_s	Masse of rock (kg)
N	Total number of rocks selected
n	Number of tests
S	Thank area (m^2)
T_{ini}	Initial rock bed temperature (°C)
T_{int}	Thank inlet temperature (°C)
T_{out}	Thank outlet temperature (°C)
T_s	Temperature of rock (°C)
V_{lit}	Volume of the thank occupied by the rocks (m^3)
V_{seg}	Volume of a segment (m^3)
V_s	Volume of a rock (m^3)
$V_{T,s}$	Total volume occupied by the rocks (m^3)

UNDER PEER REVIEW

W_p	The fan power (W)
ρ_s	Density of the rock (kg/m^3)
ε	Porosity of the rock bed
Ψ	Sphericity of the rock
η_{ch}	Charge efficiency
η_{dech}	Discharge efficiency

1. Introduction

Many studies have been conducted on solar thermal dryers in recent years, such as direct solar dryers, indirect solar dryers, hybrid solar dryers and mixed solar dryers [1]. Most of these solar dryers are highly dependent on the effective presence of solar radiation. Solar energy is a renewable energy, but it is not available at all times of the day. This unavailability of solar energy limits the applications of solar dryers. To overcome this drawback, it is necessary to add thermal energy storage devices to those of solar dryers. The storage of solar thermal energy consists of accumulating solar energy during a sunny period of the day and releasing it later for useful purposes when there is no more sun. Solar energy is a renewable source of energy and therefore a long-term alternative for many applications, including solar thermal applications such as drying, home heating etc. [2]. Due to the intermittency of solar energy, solar thermal energy systems need to be efficient and effective. Thermal energy can be stored in various forms: (i) sensible, (ii) latent or thermochemical [3]. Sensible heat storage involves increasing the temperature of the storage material without the material changing state, whereas latent heat storage involves increasing the temperature of the storage material to its change of state temperature [4]. Thermochemical heat storage is based on reversible chemical reactions and sorption phenomena [5]. Various heat storage materials have been the subject of several studies ([4], [6]-[8]). The most commonly used in heat storage are mainly water, essential oils, rocks, concrete, phase change materials (PCM), calcium and zeolite [8]. However, the choice of storage material depends on the form or type of storage used. Thus water, essential oils, rocks or concrete are generally used in sensitive storage, while phase change materials (PCMs) are used in latent storage. Thermochemical heat storage is in the laboratory phase and has not been studied extensively, but calcium, zeolite are generally used as storage materials ([4], [9]). Solar storage systems on rock beds with air as a heat transfer fluid have been studied several times ([10]-[12]). Rocks have a much lower energy storage density compared to water and PCMs due to their low heat capacity, but have a high thermal conductivity compared to PCMs [10]. To do so, the implementation of a rock bed energy storage system requires a larger storage volume [13]. However, the use of rocks as storage materials has some advantages such as low cost, availability and easy access [11]. They also have good heat transfer characteristics when used with air as the heat transfer medium [14]. In the present study, we are interested in the sensible heat storage system from the perspective of its integration into a low temperature application (less than or equal to 120°C). The objective of the present work is to evaluate through an experimental study the thermal performance of the granite bed storage system with air as heat transfer fluid and to analyse the capacity of the system to store and supply the energy necessary for a drying system.

2. Materials and methods

2.1. Materials

2.1.1 Materials for storage tank design

The choice of materials for the design of a storage tank system is very important. The material of the tank frame must be able to withstand temperatures higher than the load temperature of the tank, to avoid any expansion effect of the tank frame that may lead to a change in the porosity of the bed. The following materials were used in the construction of our storage device: a stainless steel sheet, metal tubes, glass wool and an aluminium sheet. The characteristics of these materials are given in Table 1.

Table 1: *Physical properties of tank materials*

UNDER PEER REVIEW

	Thermal conductivity	Density	Heat capacity
Stainless steel[15]	70 $W.m^{-1}.K^{-1}$	7850 $kg.m^{-3}$	478 $J.kg^{-1}.K^{-1}$
Aluminium sheet[16]	237.9 $W.m^{-1}.K^{-1}$	2702 $kg.m^{-3}$	880 $J.kg^{-1}.K^{-1}$
Glasswool[17]	0.04 $W.m^{-1}.K^{-1}$	200 $kg.m^{-3}$	670 $J.kg^{-1}.K^{-1}$

2.1.2 Storage material characterisation equipment

The role of storage material characterisation is to determine the thermo-physical properties of the material such as density, conductivity, mass heat capacity etc. To characterise the granite, the following equipment was used: (i) a graduated cylinder to determine the volume of the granite sample, (ii) an electronic balance to determine its mass and (iii) the KD2-Pro thermal analyser to determine the thermal conductivity, thermal diffusivity and specific heat of the material.

2.1.3 Storage tank performance characterisation equipment

The characterisation of the thermal performance of the storage system required the following materials and devices:

- A flat plate solar thermal collector which represents the heat source of the storage system. It acts as a solar radiation converter. It converts the incident solar energy into thermal energy;

- A fan (precision 2820 rpm, 220V, 550W and 50Hz) which ensures the forced convection of the heat transfer fluid from the collector to the storage tank;

- K-type thermocouples (measuring range: -100°C - 1370°C; accuracy ± 0.05% of reading + 1.0°C) which monitor the temperature of the rock bed in the tank and of the collector;

- A midi LOGGER GL220 data acquisition system that allows the recording and monitoring of the temporal evolution of the temperature of the rock bed in the reservoir.

2.2 Methodology

2.2.1 Characterisation of the storage material

2.2.1.1 Density determination

The density of the rocks is obtained by measuring the mass of some rock samples using an electronic balance with a capacity of 10 kg and a resolution of 0.1 kg, and by measuring the volume of these samples using a graduated tube. Into the graduated tube containing initially the volume V_i of water is added the mass of the rock sample. The value of the mixture (water plus rock) reaches the volume V_f. The difference $V_s = V_f - V_i$ represents the volume of water displaced by the sample. The operation is carried out three times and the density of the sample is obtained by averaging the ratio between the mass of the sample and the volume of water displaced by the sample by the relationship (1).

$$\rho_s = \frac{1}{n}\sum_{i=1}^{n}\frac{m_{s,i}}{V_{s,i}} \quad (1)$$

Where m_s is the mass of the sample in kg and V_s the volume of water displaced by the sample in m^3. The figure below shows the devices for measuring the density of the sample.

UNDER PEER REVIEW

Fig. 1: Density measuring device

2.2.1.2 Determination of thermal conductivity

Thermal conductivity was measured by a thermal analyser with a probe, the "KD2-Pro". The principle of the measurement is to drill a hole in the rock with a drill containing a drill bit of the same diameter as the probe of the "KD2-Pro". Before introducing the probe into the hole for measurement, it was covered with a gel (prenium ceramic polysynthetic) as well as the hole to avoid any air entry. The type of probe used for the rock characterisation is the "RK-1". The figure below shows the measurement steps. The values obtained are automatically recorded on the "KD2-Pro" memory.

Fig. 2: Thermal conductivity measurement steps: (a) Hole made in the rock, (b) Probe inserted into the hole

2.2.1.3. Determination of the average diameter of rocks

The average density of the rocks obtained by immersing a few samples was used to estimate their equivalent volume. By weighing a rock, it is possible to estimate its volume thanks to its average density calculated previously. To determine the equivalent diameter of the rocks used for storage, approximately 200 rock samples were individually weighed. The individual volume of each rock was calculated as the ratio of the mass of the rock to the density. The average diameter is thus calculated by applying equation (2), proposed by Thibaut Esence [18].

$$d_{eq} = \left(\frac{6}{\pi} \times \frac{\sum_i^N V_{s,i}}{N} \right)^{1/3} \quad (2)$$

2.2.1.4: Determination of fixed bed porosity

The porosity is defined as the fraction of void occupied by the heat transfer fluid in the rock bed. During the filling of the storage tank, the rocks were washed, dried and then weighed before being introduced into the tank. A total of 294.8 kg of rock was introduced into the tank. The porosity of the rock bed was determined by dividing the difference between the volume of the bed and the volume occupied by the rocks by the volume of the bed according to the equation below:

$$\varepsilon = \frac{V_{lit} - V_{T,s}}{V_{lit}} \quad (3)$$

Where $V_{T,s}$ is the volume occupied by the rocks in the reservoir obtained by multiplying the density of the rock by the total mass of the rocks in the reservoir and is the volume of the rock bed, V_{lit} is the volume of the reservoir occupied by the rocks and ε the porosity of the rock bed.

2.2.1.5 Determination of the sphericity of rocks

Sphericity is defined as the ratio of the surface area of the same volume sphere to the actual surface area of the solid [19]. It allows the diameter of the sphere of the same specific area to be estimated from the diameter of the sphere of the same volume according to equation (4). It can also be estimated visually using the diagram proposed by *Krumbein and Sloss* [18] (Figure 4). Figure 3 shows a photograph of our storage material and allows a comparison with the diagram of *Krumbein and Sloss* for the determination of the sphericity of our material.

$$d_{eq,a} = \Psi . d_{eq} \quad (4)$$

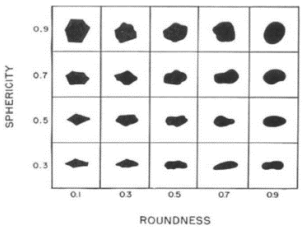

Fig.3: Diagram for visual estimation of sphericity

Fig. 4: Photo of the material used for storage

2.2.2 Construction of the storage tank

The frame of the storage system was constructed in the form of a vertical cylinder with an internal diameter of 0.6 m and a height of 1.2 m. The bottom of the tank is fitted with a sieve to retain solid particles. The storage tank is fitted with a 0.09 m diameter orifice, which allows hot air to be introduced. Seventeen pipes are distributed on either side of the tank. These small pipes, 2 cm in diameter, are spaced 10 cm apart and allow the thermocouples to be inserted along the bed. The tank is insulated with 5 cm thick glass wool and finally a corrugated sheet is used to cover the insulation.

UNDER PEER REVIEW

2.2.3 Determining the thermal performance of the tank

2.2.3.1 Stored energy

The total energy stored E_{Tch} during the rock bed loading process can be defined as the sum of the energies in each segment of the storage tank [20]. It is expressed as follows:

$$E_{Tch} = \rho_s C_{p_s} (1-\varepsilon) V_{seg} \sum_{i=1}^{n} \Delta T_i \quad (5)$$

Where V_{seg} is the volume occupied by a segment and ΔT the temperature difference between two adjacent nodes of a segment and n is the number of segments in the tank and in our case n is 7.

2.2.3.2 Charging efficiency and discharging efficiency

The charging efficiency of the storage system can be determined as the ratio of the total energy stored during the charging phase to the energy supplied to the storage system until the end of charging [21]. This definition is expressed by equation (6).

$$\eta_{ch} = \frac{\int_0^H \rho_s . C_{P_s} . S . (1-\varepsilon) . (T_s(z) - T_{ini}) . dz}{\int_0^t \dot{m}_{ch} . C_{P_a} (T_{int} - T_{ini}) . dt} \quad (6)$$

Where η_{ch} is the charging efficiency, T_{ini} the initial temperature of the rock bed, S the bed surface, $T_s(z)$ the rock temperature, C_{P_s} the specific heat of the solid, the specific heat of the air, the fluid flow rate during charging, T_{int} the inlet temperature of the heat transfer fluid, H the height of the rock bed and t the total duration of the charging phase which is 7h.

The discharge efficiency is determined as the ratio of the total energy recovered by the storage system during the discharge phase to the total energy stored during the charge phase. However, the energy input of the fan in the heat recovery process can be significant. The energy consumption of the fan during the discharge phase is added to the total energy stored in the bed ([21], [22]). As can be seen in equation (7):

$$\eta_{dech} = \frac{\int_0^{t_{dech}} \dot{m}_{dech} . C_{P_a} . (T_{out} - T_{int}) dt}{\int_0^H \rho_s . C_{P_s} . (1-\varepsilon) . (T_s(z) - T_{ini}) . S . dz + \int_0^{t_{dech}} W_p . dt} \quad (7)$$

Where $\dot{m}_{dech}$ is the mass flow rate at the tank inlet during the discharge phase, T_{out} and T_{int} respectively the outlet temperature and the tank inlet temperature during the discharge phase, W_p the fan power and the total duration of the discharge phase which is 2h20min.

3. Temperature measurement

Type K thermocouples (+1.0°C for a temperature range between 0 and 100°C) were used to control the temperature distribution along the central axis of the bed. These thermocouples were positioned so that their tips did not touch the walls of the pipe. Temperatures were measured at eight (08) different locations along the height of the tank at 0.1m intervals. The thermocouples were connected to a data acquisition system that recorded the temperature data in real time. Before data recording began, i.e. before loading began, the rock bed was blown with air at room temperature until all the thermocouples were almost at the same temperature. Figure 7 shows the experimental set-up.

UNDER PEER REVIEW

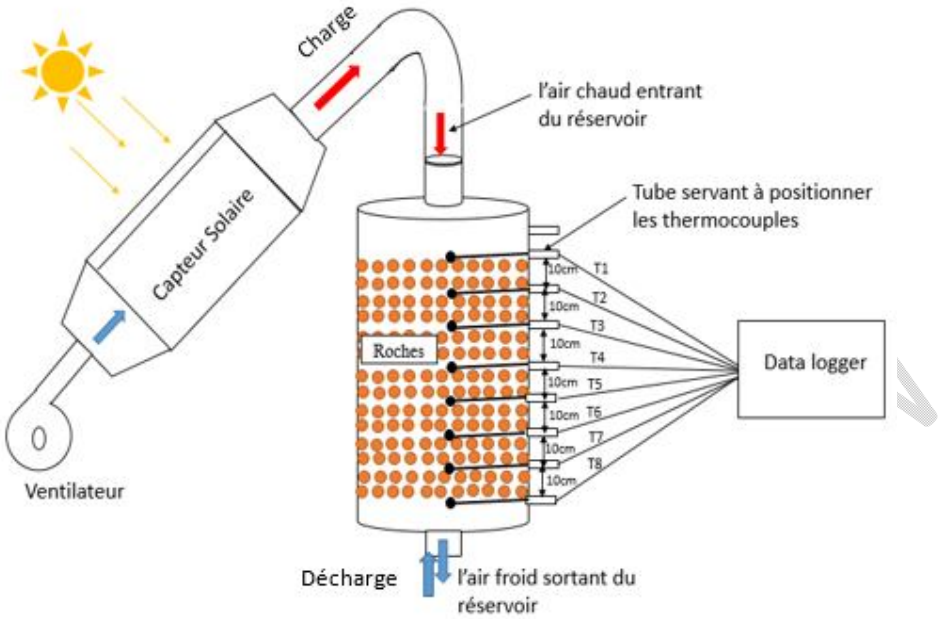

Fig. 5: Diagram showing the positioning of the thermocouples and the acquisition of the data

4. Results and discussion

4.1 Granite characteristics

Table 2 shows the physical properties of the rocks used. The specific heat of the material could not be determined. The measured physical property values are in perfect agreement with those given by Tiskantine et al [8].

Table 2: Physical properties of granite

Paramètres	Valeurs	Data from Tiskantine [8]
Heat capacity (J/kg.K)	600-950	600-950
Heat conductivity (W/m.K)	2,61	2,725
Density (kg/m^3)	2775	2659
Diameter (m)	0,0187	-
Porosity	0,53	-
Sphericity	0,7	-

The heat transfer fluid parameters calculated at the average temperature are given in Table 3 below.

Table 3: Heat transfer fluid parameters

C_{p_a}	$1000\ J.k\,g^{-1}.K^{-1}$
ρ_a	$1{,}1\ kg.m^{-3}$
$\dot{m}_{ch}$	$0{,}014\ kg.s^{-1}$
$\dot{m}_{déch}$	$0{,}021\ kg.s^{-1}$

UNDER PEER REVIEW

4.2 Tank temperature profiles during charging and discharging

The axial and temporal temperature distribution profiles during the charging and discharging phase of the storage tank are presented in figures 6.

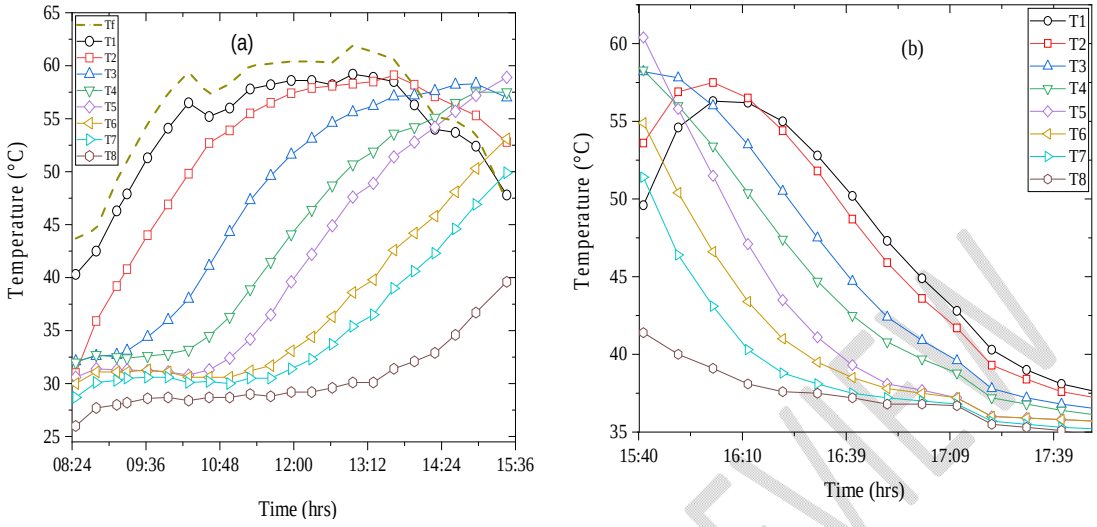

Fig. 6: Tank temperature distribution profile as a function of time during charging (a) and discharging (b)

Observation of the different bed temperatures in figure 6 (a) shows that the temperature at each node increases progressively at the start of the load at 8am depending on the sunshine and the output temperature of the solar collector until it reaches a maximum at around 12pm - 2pm. The temperature at the top of the tank remains the highest during this time. The temperature of the second node is higher than the third node and so on until the last node. The temperature of the second node is higher than the third node and so on until the last node. After 2pm, the temperature at the top of the tank gradually decreases. This is due to the decrease in the intensity of the solar energy resulting in a decrease in the air temperature at the collector outlet or in the tank inlet temperature. While the lower nodes remain unchanged during this period. This may be due to convection transfers of energy stored by the solids at the first node to the lower nodes. During the first charging period the bed is stratified, as the solar irradiance and the temperature at the collector outlet increase during this period. And during the second period, the bed gradually loses the stratification as the sunshine and the air temperature at the collector outlet decrease.

As shown in figure.6 (b), the temperature of the different nodes gradually decreases during the discharge. At the beginning of the discharge phase at 15:40 the temperature profile of the first node is lower than the other nodes except the last one. Then it gradually increases until it reaches the temperature of the second node around 16:30. This is the period during which the bed is not stratified. After 16:30 the temperature of the first node remains the highest until the end of the discharge, after which the temperature of the second node follows and so on until the last node. During this period the bed keeps its stratification until the end of the discharge.

4.3 Total energy stored, energy discharged

The total energy stored and the amount of heat supplied by the storage system during the charging and discharging process respectively are shown in figure.7.

UNDER PEER REVIEW

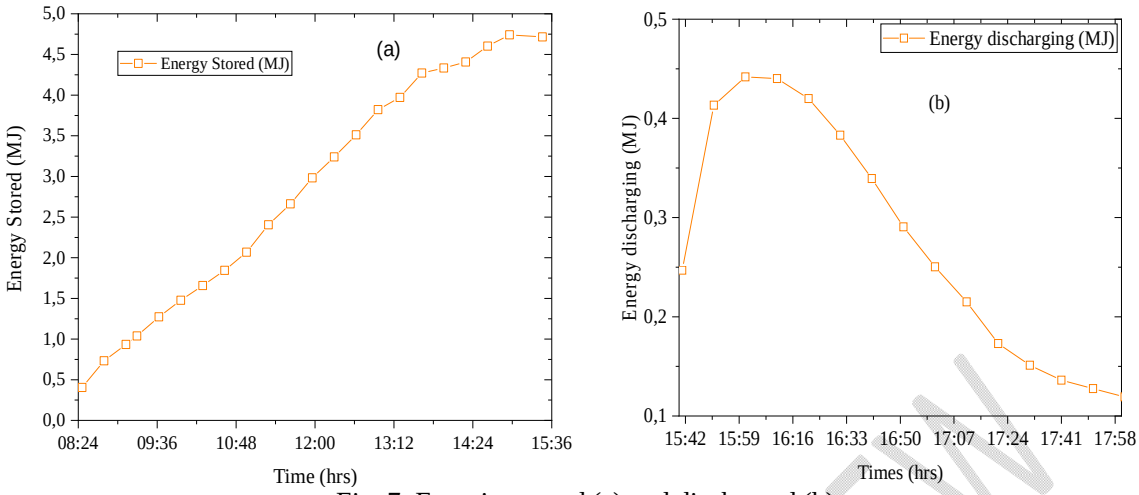

Fig. 7: Energies stored (a) and discharged (b)

The figure 7.(a) shows that the energy stored during charging increases gradually over the course of the day, reaching its maximum between 14:30 and 15:36 where it stabilises. This shows that between 8am and 3pm the system stores a significant amount of energy of 4.71M J.

As can be seen in figure 7 (b), the amount of heat supplied by the storage during the discharge process increases gradually until it reaches a maximum value of 0.45 MJ at about 16.10 h and then it decreases gradually until the end of the discharge. The period when the heat supplied by the system is maximum corresponds to the period when the temperature of the first node is at its maximum during the discharge phase. The total amount of heat supplied by the system during this phase is 4.14 MJ.

4.4 Charge phase efficiency, discharge phase efficiency and overall efficiency

The efficiency can be seen as a measure of the thermal stratification of the storage system. The higher the efficiency, the better the stratification of the system. The efficiency obtained during the different phases and the overall efficiency of the system are recorded in Table 4 below. The efficiency value obtained during the charging phase of 76.8%, coincides with that obtained by Singh et al[2], who obtained an average efficiency value between 75-77% in a study on the thermal performance of a packed bed solar storage system for solar air heaters. But it is still lower than that obtained by Ahmet Kurklu et al [24], who obtained an efficiency value of 80% for a solar storage system for heating a greenhouse. This may be due to heat losses to the outside of the storage system during the charging process or to the physical properties of the material used in their study $C_p = 800\ J/kg.K$ *et* λ*=2,9 W/m.K* which are superior to those used in our study, which are de $C_p = 775\ J.kg^{-1}.K^{-1}$ *et* λ*=2,61* $W.m^{-1}.K^{-1}$.

Table 4: Results of different efficiencies and total stored and discharged energy

Charging time	7h
Discharging time	2h20mn
Total energy stored	4,7 MJ
Total discharged energy	4,14 MJ
Charging efficience	76,8%
Discharging efficience	44,4%

5 Conclusion

An experimental setup was presented to study the thermal performance of a sensitive solar storage system with granite as storage material and air as heat transfer fluid. The results obtained show that

UNDER PEER REVIEW

the storage system is most suitable for solar dryers, as the bed temperature increased from an initial average temperature of 36.5°C to a maximum temperature of 63.7°C during the day and the charging efficiency was 76.8% which is in full agreement with the literature. The results show that more than 80% of the total stored energy is recovered during the discharge phase, demonstrating a good performance of the storage system. The solar energy loses its power during the day and this negatively affects the thermal energy storage process in the rock bed during the charging phase, resulting in a decrease in the stored thermal energy and thus a decrease in the thermal performance of the storage system. An optimal shutdown time of the charging phase must therefore be sought in order to preserve the stored thermal energy. In addition, a detailed study of the tank discharge time is required, as a too short discharge time after sunset can have a negative impact on certain products to be dried.

References

[1] C. Aboubacar, "Energy study of a solar-gas hybrid dryer for onion drying applications "Violet de Galmi", OUAGA UNIVERSITY I PROFESSOR JOSEPH KI-ZERBO, 2016.

[2] P. L. Singh, S. D. Deshpandey, and P. C. Jena, "Thermal performance of packed bed heat storage system for solar air heaters," Energy Sustain. Dev, vol. 29, p. 112-117, 2015, doi: 10.1016/j.esd.2015.10.010.

[3] J.A. Duffie and W.A. Beckman, "Solar Engineering of Thermal Process." p. 893, 2006.

[4] N. Mahfoudi, "Heat storage in a solid granular medium," Mohamed Khider University - Biskra, 2016.

[5] L. Farcot, "Study of a thermochemical heat storage system with separate reactor", UNIVERSITE GRENOBLE ALPES Spécialité, 2019.

[6] J.-F. HOFFMANN, "Thermal storage for concentrated thermodynamic solar power plant using natural or recycled materials," UNIVERSITY OF PERPIGNAN VIA DOMITIA, 2015.

[7] K. N. E. Serge, "LOCAL ECO-MATERIAL-BASED THERMAL STORAGE FOR CONCENTRATION SOLAR POWER PLANTS: CASE OF THE CSP4AFRICA PILOT," UNIVERSITY OF PERPIGNAN VIA DOMITIA, 2017.

[8] R. TISKATINE, "Energy valorization of local materials for applications in CSP plants and buildings," IBN ZOHR UNIVERSITY, 2017.

[9] S. Hongois, "Inter-seasonal thermochemical heat storage for solar heating of individual houses," L'Institut National des Sciences Appliquées de Lyon, 2012.

[10] D. Okello, C. W. Foong, O. J. Nydal, and E. J. K. Banda, "An experimental investigation on the combined use of phase change material and rock particles for high temperature (~350 C) heat storage", Energy Convers. Manag., vol. 79, p. 1-8, 2014, doi:10.1016/j.enconman.2013.11.039.

[11] H. Singh, R. P. Saini, and J. S. Saini, “A review on packed bed solar energy storage systems,” Renew. sustain. Energy Rev., vol. 14, no. 3, p. 1059-1069, 2010, doi:10.1016/j.rser.2009.10.022.

[12] D. L. Zhao, Y. Li, Y. J. Dai and R. Z. Wang, "Optimal study of a solar air heating system with pebble bed energy storage", Energy Convers. Manag., vol. 52, no. 6, p. 2392-2400, 2011, doi:10.1016/j.enconman.2010.12.041.

[13] R. Daschner, S. Binder and M. Mocker, "Pebble bed regenerator and storage system for high temperature use", Appl. Energy, vol. 109, p. 394-401, 2013, doi: 10.1016/j.apenergy.2012.10.062.

[14] Hans W. Fricker, "High-temperature heat storage using natural rock," Sol. Energy Mater., vol. 24, p. 249-254, 1991.

[15] G. L. SAWADOGO, "Modeling of heat transfer phenomena in an insulated oven with local materials: Application to the energy optimization of meat grilling equipment", JOSEPH KI-ZERBO UNIVERSITY, 2020.

UNDER PEER REVIEW

[16] D. A. Oumar, "CONVECTIVE DRYING OF MANGO: ANALYSIS OF THE INFLUENCE OF AERAULIC AND INTRINSIC PARAMETERS, DESIGN AND MODELING OF THE OPERATION OF AN INDIRECT SOLAR DRYER", UNIVERSITY OF OUAGADOUGOU, 2007.

[17] A. O. Dissa, J. Bathiebo, S. Kam, P. W. Savadogo, H. Desmorieux, and J. Koulidiati, "Modelling and experimental validation of thin layer indirect solar drying of mango slices," Renew. Energy, vol. 34, no. 4, p. 1000-1008, 2009, doi:10.1016/j.renene.2008.08.006.

[18] T. ESENCE, "Study and modeling of solid/fluid regenerative thermal storage systems", UNIVERSITY GRENOBLE ALPES, 2017.

[19] H. Wadell, "Volume, shape, and roundness particles", J. Geol. flight. 40, no. 5, p. 443-451, 1932.

[20] A. Mawire, M. McPherson, R.R.J. den Heetkamp, and S. J. P. Mlatho, "Simulated performance of storage materials for pebble bed thermal energy storage (TES) systems," Appl. Energy, vol. 86, no. 7-8, p. 1246-1252, 2009, doi: 10.1016/j.apenergy.2008.09.009.

[21] G. Türkakar, "Performance analysis and optimal charging time investigation of solar air heater with packed bed sensible heat storage device," Sol. Energy, vol. 224, no. June, pp. 718-729, 2021, doi: 10.1016/j.solener.2021.06.007.

[22] S. Kuravi, J. Trahan, D. Y. Goswami, M. M. Rahman and E. K. Stefanakos, "Thermal energy storage technologies and systems for concentrating solar power plants", Prog. Energy Fuel. Science, vol. 39, no. 4, p. 285-319, 2013, doi:10.1016/j.pecs.2013.02.001.

[23] D. K. Kedida, D. A. Amibe and Y. T. Birhane, "Performance of a Pebble Bed Thermal Storage Integrated with Concentrating Parabolic Solar Collector for Cooking," J. Renew. Energy, vol. 2019, p. 1-12, 2019, doi: 10.1155/2019/4238549.

[24] A. Kürklü, S. Bilgin, and B. Özkan, "A study on the solar energy storing rock-bed to heat a polyethylene tunnel type greenhouse," Renew. Energy, vol. 28, no. 5, p. 683-697, 2003, doi: 10.1016/S0960-1481(02)00109-X.

UNDER PEER REVIEW